

## INFLUENCE OF STRESS-STIFFENING ON THE DYNAMIC BEHAVIOUR OF PLATES: DIRECT AND INVERSE PROBLEMS

### Domingos Alves Rade

Federal University of Uberlândia – School of Mechanical Engineering  
domingos@ufu.br

### Alberto Borges Vieira Jr.

Federal University of Bahia – Department of Mechanical Engineering  
abvieira@ufba.br

### Jhojan Enrique Rojas Flores

Federal University of Uberlândia – School of Mechanical Engineering  
jerojas@mecanica.ufu.br

### Alexandre Campos Bezerra

Federal University of Uberlândia – School of Mechanical Engineering  
acbezerra@mecanica.ufu.br

**Abstract.** *It is widely known that the presence of mechanical stresses can have a significant influence on the static and dynamic behavior of structural components, due to the so called stress-stiffening effect. As a complement to studies previously published by the authors, in this paper the influence of normal and shear membrane stresses on the dynamic behavior of thin rectangular plates is addressed, emphasis being placed on two particular aspects: a) the numerical characterization of the influence of membrane stresses on the natural frequencies associated to the bending modes; b) the possibility of identifying applied in-plane external loads given a set of experimentally-measured natural frequencies associated to bending modes. The underlying theory is first presented including the development of a low-order mathematical model for the flexural vibrations of plates subjected to in-plane loads, based on Kirchhoff's theory and the assumed modes method. Then, the parameterization of the stress field is discussed and the use of polynomial approximations for the Airy's stress function is suggested. A parameter identification problem is formulated in such a way that the stress distributions – or alternatively, the external loads – are identified by solving an optimization problem in which the cost function represents the deviations between the values of the natural frequencies of the loaded plate and their model-predicted counterparts. The results of numerical simulations and experiments are presented to illustrate some of the main aspects of the study.*

**Keywords:** *stress-stiffening, Kirchhoff Plates, Inverse Problems, Assumed Modes*

### 1. Introduction

The so called *stress-stiffening* effect is characterized by the fact that when subjected to a given stress field, structural components such as strings, beam and plates exhibit variations in their bending stiffness and, as a result, modifications in their static and dynamic behavior. Such phenomenon is observed in the presence of stress fields generated either by external loading or by self-equilibrating residual stresses that can be produced by various thermo-mechanical manufacturing processes such as welding and cold-forming.

A number of studies have been reported in the literature focusing the stress-stiffening effect in connection with the static or dynamic structural behavior of structural components. Simons and Leissa (1971) used the Rayleigh-Ritz approach to investigate the influence of in-plane acceleration loads on the natural frequencies of rectangular cantilever plates. The same method, combined with the use of beam characteristic functions in the deflection series was used by Kaldas and Dickinson (1981) to characterize the influence of various types of stress distributions on the vibration and buckling behavior of rectangular plates. Donadon *et al.* (2002) investigated numerically and experimentally the effect of in-plane stresses induced by piezoelectric actuators on the natural frequencies of composite plates. More recently, the effect of non-uniform in-plane thermal stresses on the vibration and buckling behavior of rectangular plates was studied numerically by Mead (2003). Rojas (2004) carried-out a comprehensive study about the stress-stiffening effect on the dynamic behavior of two-dimensional frames and rectangular plates, considering both direct and inverse problems. Greening and Lieven (2001) demonstrated experimentally the variability in the dynamic responses of nominally identical structures, due to residual stresses introduced through manufacturing processes. The same authors developed a strategy for including the stress-stiffening effect in a model updating procedure intended for the identification of the axial loads acting on the member of two-dimensional frames. In a similar approach, Rojas *et al.* (2004) used heuristic optimization methods for the identification of external loads in frames. Most of these studies demonstrated the strong influence the stress-state can have upon the dynamic characteristics of vibrating systems, leading to conclude that in many circumstances, the stress-stiffening effect must be taken in account in the modeling procedures so as to guarantee the accuracy of model predictions.

This paper is devoted to a feasibility study of a methodology for the identification of external in-plane loads applied to rectangular plates, given a set of natural frequencies corresponding to bending modes of the loaded plate and a mathematical model relating such frequencies with the loading. An *inverse problem* is formulated in such a way that the unknown loading parameters are identified by solving a nonlinear constrained optimization problem. In the remainder, various aspects related to the identification method are discussed, including the underlying theory and the results obtained from numerical simulations and laboratory tests.

## 2. Modeling of Flexural Vibrations of Thin Plates Subjected to Membrane Stresses by the Assumed-Modes Approach

Figure 1 illustrates a uniform rectangular plate of dimensions  $a \times b \times h$ , being also depicted an element which is acted upon by normal and shear stress components  $\sigma_x, \sigma_y$  and  $\tau_{xy}$ .

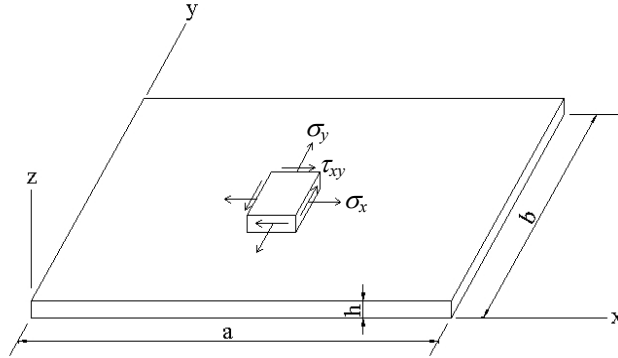


Figure 1. Stress components applied to an element of the plate

According to Kirchhoff's plate theory, the following assumptions are adopted:

- plate thickness is small and constant. External faces are parallel to the middle plane, which is assumed to coincide with  $x$ - $y$  plane;
- cross-sections remain plane and perpendicular to the middle plane after deformation;
- plane stress state is assumed, transverse shear stresses being neglected.

Neglecting dissipation effects, the Assumed-Modes Method (Craig Jr., 1981) is used to derive a discrete model for the flexural vibrations of the plate, taking into account the membrane stresses. With this aim, the kinetic and strain energies of the plate are first written as follows (Géradin and Rixen, 1997):

$$T(t) = m \int_0^b \int_0^a \left( \frac{\partial w}{\partial t} \right)^2 dx dy \quad (1)$$

$$U(t) = \frac{1}{2} \int_0^b \int_0^a \left\{ D \left( \frac{\partial^2 w}{\partial x^2} + \frac{\partial^2 w}{\partial y^2} \right)^2 - 2D(1-\nu) \left[ \frac{\partial^2 w}{\partial x^2} \frac{\partial^2 w}{\partial y^2} - \left( \frac{\partial^2 w}{\partial x \partial y} \right)^2 \right] \right\} dx dy$$

$$+ \frac{1}{2} h \int_0^b \int_0^a \left[ \sigma_x \left( \frac{\partial w}{\partial x} \right)^2 + \sigma_y \left( \frac{\partial w}{\partial y} \right)^2 + 2\tau_{xy} \frac{\partial w}{\partial x} \frac{\partial w}{\partial y} \right] dx dy \quad (2)$$

where:

- $w = w(x, y, t)$ : transverse displacement field
- $m$ : mass density of the plate (mass per unit area)
- $\nu$ : Poisson's ratio
- $D = Eh^3 / [12(1-\nu^2)]$ : plate flexural stiffness
- $E$ : Young modulus

According to the Assumed-Modes Method, the plate transverse displacement field is expressed as a truncated linear combination of arbitrarily selected admissible functions. Following the approach adopted by Kaldas and Dickinson (1981), these functions are chosen to be the eigenfunctions of vibrating beams satisfying the geometrical boundary conditions of the plate in directions  $x$  and  $y$ . Thus, one writes:

$$w(x, y, t) = \sum_{i=1}^p \sum_{j=1}^q q_{ij}(t) \phi_i(x) \psi_j(y) \quad (3)$$

where  $p$ ,  $q$  are the numbers of eigenfunctions considered in the series in  $x$  and  $y$  directions, respectively;  $q_{ij}(t)$  are unknown generalized coordinates and  $\phi_i(x)$  and  $\psi_j(y)$  designate the beam eigenfunctions which are expressed as combinations of trigonometric and hyperbolic functions as follows (Young, 1950):

$$\phi_i(x) = A_i \sin\left(\eta_i \frac{x}{a}\right) + B_i \cos\left(\eta_i \frac{x}{a}\right) + C_i \sinh\left(\eta_i \frac{x}{a}\right) + D_i \cosh\left(\eta_i \frac{x}{a}\right) \quad (4.a)$$

$$\psi_j(y) = E_j \sin\left(\xi_j \frac{y}{b}\right) + F_j \cos\left(\xi_j \frac{y}{b}\right) + G_j \sinh\left(\xi_j \frac{y}{b}\right) + H_j \cosh\left(\xi_j \frac{y}{b}\right) \quad (4.b)$$

In equations (4),  $A_i, B_i, C_i, D_i, \eta_i, E_j, F_j, G_j, H_j, \xi_j$  are constant coefficients that depend on the boundary conditions. Young (1950) provides the numerical values of these coefficients for three combinations of boundary conditions: *clamped-clamped*, *clamped-free* and *free-free*.

To avoid unnecessary complication in the notation, the expansion expressed by Equation (3) is rewritten as follows:

$$w(x, y, t) = \sum_{k=1}^N C_k(t) \eta_k(x, y) \quad (5)$$

where:

- $C_k(t) = q_{ij}(t)$
- $\eta_k(x, y) = \phi_i(x) \psi_j(y)$
- $N = p \times q$
- $k = (j-1)p + i$

Introducing matrix notation, Eq. (5) is written:

$$w(x, y, t) = \{\eta(x, y)\}^T \{C(t)\} \quad (6)$$

where:

$$\{\eta(x, y)\} = [\eta_1(x, y) \quad \eta_2(x, y) \quad \cdots \quad \eta_N(x, y)]^T \quad (7.a)$$

$$\{C(t)\} = [C_1(t) \quad C_2(t) \quad \cdots \quad C_N(t)]^T \quad (7.b)$$

Upon introduction of Equation (6) into equations (1) and (2), the following expressions for the kinetic and strain energies are obtained:

$$T(t) = \frac{I}{2} \{\dot{C}(t)\}^T [M] \{\dot{C}(t)\} \quad (8)$$

$$U(t) = \frac{I}{2} \{C(t)\}^T [K] \{C(t)\} \quad (9)$$

where:

$$[M] = \rho h \int_0^b \int_0^a \{\eta(x, y)\} \{\eta(x, y)\}^T dx dy \quad (10)$$

and

$$[K(\{\sigma\})] = [K_1] + [K_2(\{\sigma\})] \quad (11)$$

with:

$$[K_1] = \int_0^b \int_0^a D \left[ \eta_{xx} \{\eta_{xx}\}^T + \eta_{yy} \{\eta_{yy}\}^T + 2\nu \eta_{xx} \{\eta_{yy}\}^T + 2(1-\nu) \eta_{xy} \{\eta_{xy}\}^T \right] dx dy \quad (12)$$

$$[K_2(\{\sigma\})] = \int_0^b \int_0^a \left[ \sigma_x \{\eta_x\} \{\eta_x\}^T + \sigma_y \{\eta_y\} \{\eta_y\}^T + 2\tau_{xy} \{\eta_x\} \{\eta_y\}^T \right] dx dy \quad (13)$$

In the equations above, the indices indicate partial derivatives of the products of beam functions with respect to the corresponding space variables and  $\{\sigma\} = [\sigma_x \quad \sigma_y \quad \tau_{xy}]^T$  indicates the vector of the stress components.

It should be pointed out that the influence of the membrane stresses on the plate dynamics appear in matrix  $[K_2(\{\sigma\})]$  which is referred to as *initial-stress stiffness* or *geometric stiffness matrix*. As can be seen in Equation (13), this matrix is a linear function of the stress components.

To obtain the differential equations of motion, Lagrange equations are used:

$$\frac{\partial L}{\partial \{C(t)\}} - \frac{d}{dt} \left( \frac{\partial L}{\partial \{\dot{C}(t)\}} \right) = \{0\} \quad (14)$$

where the Lagrangian function is defined as:

$$L = T - U = \frac{1}{2} \{\dot{C}(t)\}^T [M] \{\dot{C}(t)\} - \frac{1}{2} \{C(t)\}^T [K(\{\sigma\})] \{C(t)\} \quad (15)$$

By introducing (15) into (14) and performing the indicated derivations, one obtains:

$$[M] \{\ddot{C}(t)\} + [K(\{\sigma\})] \{C(t)\} = \{0\} \quad (16)$$

which represents a  $N$  d.o.f. discrete model for the flexural vibrations of the plate accounting for the membrane stresses.

Equations (16) can be numerically solved for the generalized coordinates  $\{C(t)\}$  and then the transverse displacement field of the plate expressed in physical coordinates can be obtained by introducing the computed generalized coordinates back in Equation (5), for a selected set of coordinates  $(x, y)$ .

From equation (16), the following eigenvalue problem is formulated:

$$([K(\{\sigma\})] - \lambda_r [M]) \{C_r\} = \{0\} \quad (17)$$

Once solved this problem, the eigenvalues  $\lambda_r$  provide the natural frequencies of the plate ( $\lambda_r = \omega_r^2$ ) and the eigenvectors  $\{C_r\}$ , after back transformation into physical coordinates through equation (13), provide the corresponding vibration mode shapes.

Besides the eigensolutions, the frequency response functions can be calculated from the mass and stiffness matrices obtained through the Assumed Modes Method. For this, harmonic variation with frequency  $\omega$  for the transversal distributed load and displacements is assumed, as indicated in the following equations:

$$P(x, y, t) = \bar{P}(x, y) e^{i\omega t} \quad (18.a)$$

$$\{C(t)\} = \{\bar{C}\} e^{i\omega t} \quad (18.b)$$

$$w(x, y, t) = \bar{W}(x, y)e^{i\omega t} \quad (18.c)$$

where the functions  $\bar{P}(x, y)$  and  $\bar{W}(x, y)$  indicate the spatial distribution of the lateral load and displacement, respectively. By combining equations (6), (18.b) and (18.c), one writes:

$$\bar{W}(x, y) = \eta(x, y)\{\bar{C}\} \quad (19)$$

The generalized forces associated to the transversal load are defined as follows:

$$\{Q(t)\} = \{\bar{Q}\}e^{i\omega t} \quad (20)$$

with:

$$\{\bar{Q}\} = \int_0^b \int_0^a \bar{P}(x, y)\eta(x, y)dx dy \quad (21)$$

After some algebraic manipulation, it can be found that the relation between the amplitudes of the generalized forces and the amplitudes of the generalized coordinates is expressed as:

$$\{\bar{C}\} = ([K] - \omega^2[M])^{-1}\{\bar{Q}\} \quad (22)$$

The harmonic responses in terms of physical coordinates observed in a set of  $c$  points of the plate identified by their coordinates  $(x_1, y_1), (x_2, y_2), \dots, (x_c, y_c)$  are obtained by using the coordinate transformation (6):

$$\{\bar{W}\} = [H(\omega)]\{\bar{Q}\} \quad (23)$$

where:

$$[H(\omega)] = [\bar{\eta}]^T ([K] - \omega^2[M])^{-1} [\bar{\eta}] \quad (24.a)$$

$$[\bar{\eta}] = [\{\eta(x_1, y_1)\} \ \{\eta(x_2, y_2)\} \ \dots \ \{\eta(x_c, y_c)\}] \quad (24.b)$$

The formulation developed above puts in evidence the fact that the presence of membrane stresses do influence the static and dynamic flexural behaviour of the plate. Clearly, the accuracy of the numerical model obtained from the Assumed Modes Method depends on the number of beam eigenfunctions used in the expansion (3).

Considering the dependency of the dynamic responses on the stress state (or, alternatively, on the external load), one is lead to consider the possibility of assessing the magnitudes and/or distributions of the stress components (or the external loading), given a set of measured natural frequencies of a loaded plate. The feasibility of such an inverse approach is examined in the next sections.

### 3. Modeling of stress fields using Airy's stress functions

In the context of the identification procedure focused in this paper, it is convenient to express the stress field over the plate in terms of a small number of parameters. A suitable model of the in-plane stress distribution can be obtained by using an Airy's stress function  $U(x, y)$  defined so as to satisfy (Timoshenko and Goodier, 1980):

$$\sigma_x = \frac{\partial^2 U}{\partial y^2}; \quad \sigma_y = \frac{\partial^2 U}{\partial x^2}; \quad \tau_{xy} = -\frac{\partial^2 U}{\partial x \partial y} \quad (25)$$

The stress components  $\sigma_x$ ,  $\sigma_y$  and  $\tau_{xy}$  must satisfy the compatibility and equilibrium conditions. Neglecting body-forces, these conditions are satisfied if, at each and every point of the plate, the following relation holds:

$$\nabla^4(U) = 0 \quad (26)$$

Various types of functions can be used as Airy's stress functions, such as trigonometric, hyperbolic and polynomial functions. In this study, polynomials have been adopted, as follows:

$$U(x, y) = C_{00} + C_{10}x + C_{01}y + C_{11}xy + C_{12}xy^2 + C_{21}x^2y + \dots \quad (27)$$

By associating equations (13), (17), (25), (26) and (27), the influence of the stress field on the plate natural frequencies and frequency response functions can be expressed in terms of a finite set of polynomial coefficients  $C_{ij}$ . Hence, having adopted an adequate polynomial, the stress identification problem consists in determining the values of the coefficients appearing in (27). Clearly, those coefficients are not all independent since equation (26) must be satisfied.

#### 4. Modeling of stress fields using a priori knowledge about stress distributions

In many circumstances, it may be difficult, or even impossible, to model with sufficient accuracy the stress state of the plate using low-order polynomials to represent the corresponding Airy's stress functions. In the case of plates subjected to external loads, a simplified approach can be devised, which consists in using a base-line finite element model by assuming that the actual distribution of external loads is known *a priori* and only their magnitudes are unknown. Such magnitudes are thus considered as the load parameter to be determine. Following this approach, equation (13) is re-written as follows:

$$[K_2] = \mathfrak{S} \int_0^b \int_0^a \left[ \sigma'_x \{\eta_x\} \{\eta_x\}^T + \sigma'_y \{\eta_y\} \{\eta_y\}^T + 2\tau'_{xy} \{\eta_x\} \{\eta_y\}^T \right] dx dy \quad (28)$$

where  $\sigma'_x$ ,  $\sigma'_y$  and  $\tau'_{xy}$  are the stress components computed from the finite element model submitted to an arbitrary external load and  $\mathfrak{S}$  is the load factor to be determine.

#### 5. Stress identification as an optimization problem

Stress (or load) identification is dealt with by formulating a constrained optimization problem in which the design variables are the parameters featuring in the model the stress distributions (either the coefficients of the polynomial representing the Airy's stress function or the load factor defined in the previous section). In this paper, it was adopted a cost function representing the dimensionless difference between the values of the measured natural frequencies of the loaded plate and those predicted by the Assumed-Modes model, described in Section 2.

Thus, the optimization problem is formulated as follows:

$$\min_{\{p\}} J = \frac{1}{\bar{\omega}} \sum_{p=1}^{nb\_freq} W_p \left[ \omega_p^{(m)} - \omega_p^{(c)}(\{p\}) \right] \quad (29)$$

$$\bar{\omega} = \frac{1}{nb\_freq} \sum_{i=1}^{nb\_freq} \omega_i^{(m)}$$

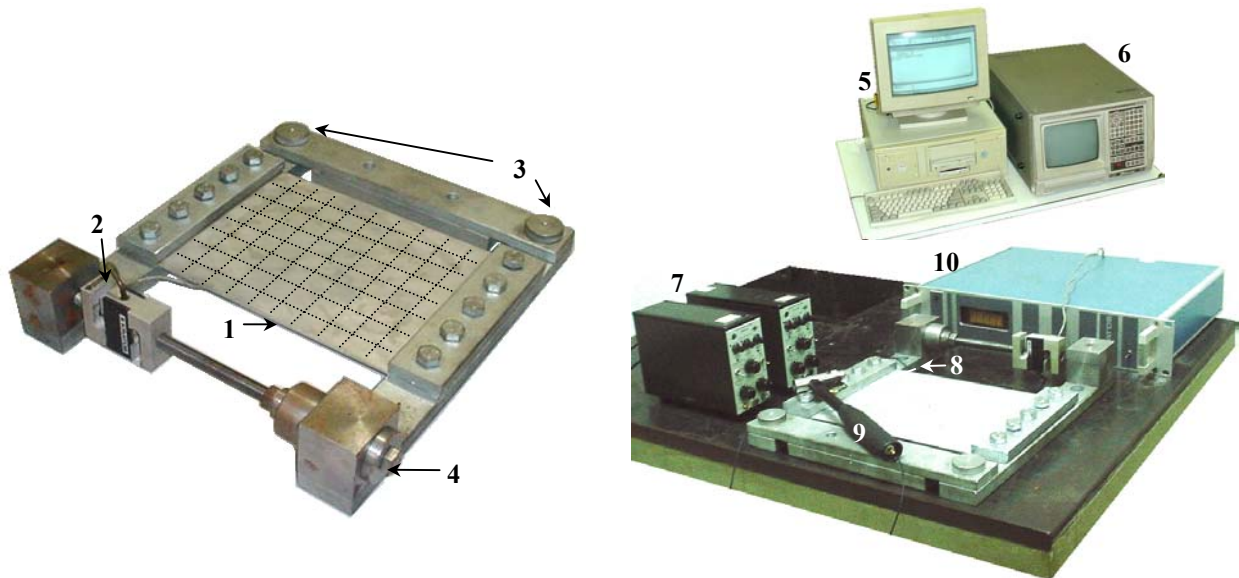
where  $\{p\}$  designates, generically, the set of unknown stress or load parameters,  $nb\_freq$  is the number of natural frequencies used for identification,  $W_p$  are user-defined weighting factors and  $\omega_p^{(m)}$  and  $\omega_p^{(c)}$  designate the measured and calculated values of the natural frequencies, respectively.

Lateral constraints are introduced to limitate the stress levels to feasible domains, accounting for material yielding and buckling, for instance.

#### 6. Experiments

The load identification procedure was evaluated by using experimental data obtained from laboratory tests performed on a rectangular plate made of aluminum, subjected to a specially designed fixture which acts also as a loading device (Figure 2). The plate was attached to the fixture in such a way to simulate clamped-clamped-free-free boundary conditions. A non-uniform in-plane traction (either tension or compression) could be applied to the plate by means of a bolt and the force could be measured through a load cell. For a given value of the applied load, vibration tests to determine the frequency response functions related to the bending vibrations of the loaded plate were carried-out. The basic components of the experimental setup are illustrated in Figure 2.

The vibration tests were performed for different values of the applied load, either in tension or compression. For each value of the load, a set of frequency responses were obtained by processing the Fourier-transformed input (impact forces) and output (transverse accelerations). The amplitudes of one of these, a driving-point FRF, corresponding to the load  $P = 190.3 \text{ N}$ , are illustrated in Figure 3, as compared to the amplitudes of the same FRF of the plate under the unloaded condition. In this figure one can evaluate the influence of the in-plane loading on the natural frequencies of the plate. Table 1 provides the values of the first six natural frequencies for both conditions, as well as the relative variations caused by loading. It can be noticed that, since the applied load is tensile, the general trend observed is the increase of the values of the natural frequencies, meaning that the plate becomes stiffer in bending, as a result of the stress-stiffening effect. The sensitivity of the natural frequencies with respect to the load varies from one mode to the other. It was found, from numerical simulations, that for a given mode such sensitivity is related to the amount of bending deformation exhibited in the direction of loading.



1-Plate; 2-Load cell; 3-Pivot points; 4-Loading bolt; 5-Microcomputer; 6-Dual-channel frequency analyser; 7-Charge amplifiers; 8-Piezoelectric accelerometer; 9- Modal hammer instrumented with load cell; 10-Signal conditioner.

Figure 2. Scheme of the plate, fixture and loading device and experimental setup of the vibration tests

Table 1. Values of the natural frequencies of the plate under unloaded and loaded condition (Hz).

	1	2	3	4	5	6
<b>Unloaded</b>	113.75	152.50	290.00	322.50	368.75	533.75
<b>Loaded</b>	126.25	158.75	302.50	328.75	370.00	541.25
<b>Variation (%)</b>	10.99	4.10	4.31	1.94	0.34	1.41

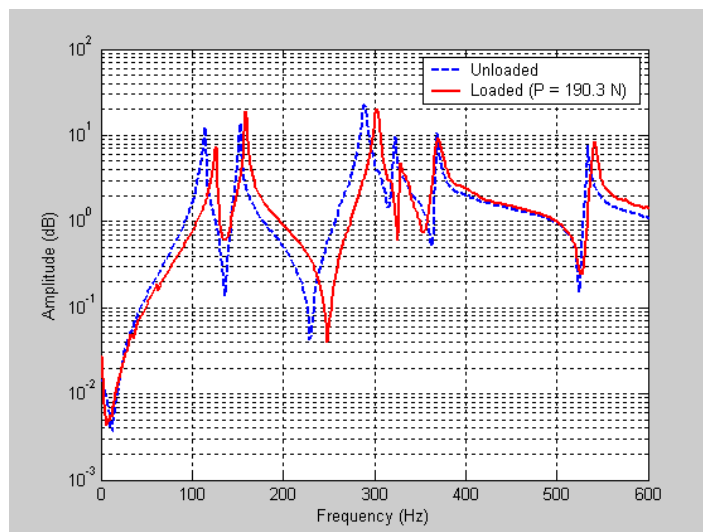


Figure 3. Amplitudes of a driving-point FRFs of the unloaded and loaded plate

## 7. Modeling of stress distribution

For the purpose of loading identification, it was adopted the following simplified model, also illustrated in Figure 4(a), for the load distribution along the clamped borders of the plate, in which  $\sigma_1$  and  $\sigma_2$  are assumed to be unknown. According to this simplified model, the stress distribution over the plate is the following:

$$\sigma_x(x, y) = \sigma_1 + \frac{\sigma_2 - \sigma_1}{b} y \quad \sigma_y(x, y) \equiv 0 \quad \tau_{xy}(x, y) \equiv 0 \quad (30)$$

By imposing the equilibrium of moments about the pivot joints of the fixture's arms, as illustrate in Figure 4(b), the following relation between the applied force and parameters  $\sigma_1$  and  $\sigma_2$  is obtained:

$$P = \frac{\frac{h(\sigma_2 - \sigma_1)b}{2} \left( \frac{2b}{3} + d_1 \right) + h\sigma_1 b \left( \frac{b}{2} + d_1 \right)}{d_1 + d_2 + b} \quad (31)$$

It can thus be seen that two parameters ( $\sigma_1, \sigma_2$ ) are to be determined, enabling to fully characterize the stress-state of the plate, according to (30). Subsequently, the applied external load  $P$  can be estimated according to (31) and the estimated value can then be compared to the exact one provided by the load cell.

However, an important question that arises concerns the accuracy of the model expressed by equations (30) in representing the actual stress-distribution of the plate. To evaluate this point, a detailed finite element model of the system plate-*fixture*, with an applied load  $P = 710$  N, has been developed to obtain a reasonably accurate description of the actual stress distributions, which are depicted in Figure 5. As can be seen, the assumption of a linearly varying distribution of  $\sigma_x$  and null values of  $\sigma_y$  and  $\tau_{xy}$  holds for the major portion of the plate, except in the vicinity of its clamped borders, where stress gradients introduced by the boundary conditions take place. Nonetheless, the magnitudes of  $\sigma_y$  and  $\tau_{xy}$  are much lower than those of  $\sigma_x$ . It is then believed that the simplified model of stress distribution (30) is adequate for identification purposes. As an additional check, the natural frequencies of the plate subjected to the simplified stress state were computed using the Assumed Modes Approach described in Section 2 and compared to their counterparts computed from the detailed finite element model, as shown in Table 2. It can be seen that the values of the two sets of frequency values are very close, demonstrating that the boundary effects have little influence on the dynamic behavior of the plate in the frequency band of interest and confirming the adequacy of the simplified model of stress distribution adopted.

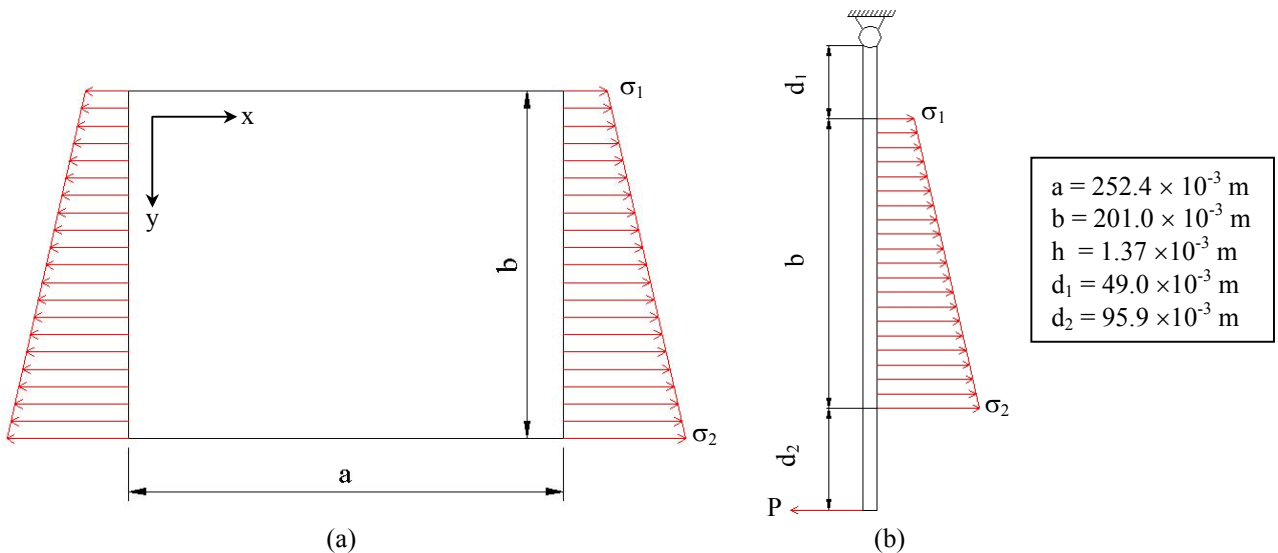


Figure 4. (a) model for the load distribution along the clamped edges; (b) free-body-diagram of the fixture arm



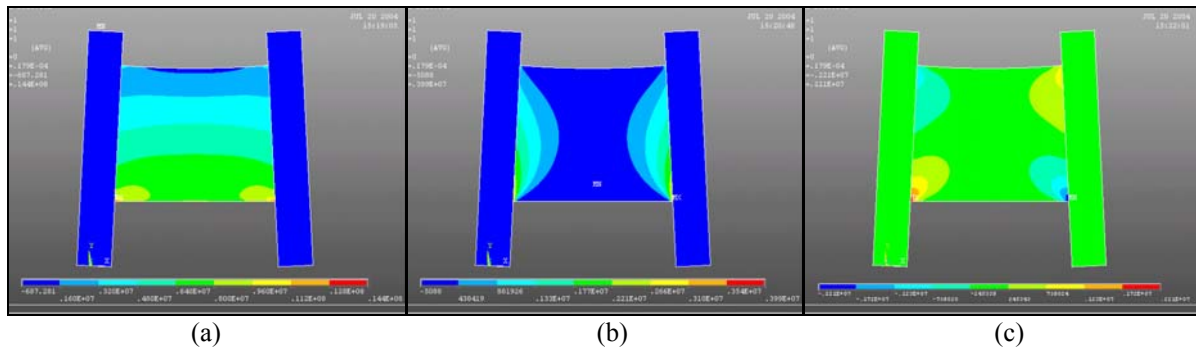


Figure 5. Stress distributions obtained from the FE model (a)  $\sigma_x$ ; (b)  $\sigma_y$ ; (c)  $\tau_{xy}$

Table 2. Values of the natural frequencies predicted by the FE and Assumed-Modes models

	Frequencies (Hz)					
	1	2	3	4	5	6
<b>Detailed FE model</b>	141.53	174.77	303.42	355.44	408.74	555.90
<b>Simplified model + Assumed Modes Method</b>	141.88	175.81	303.99	356.08	410.14	556.07
<b>Deviations (%)</b>	0.25	0.60	0.19	0.18	0.34	0.03

## 8. Load identification

Initially, the identification procedure was applied to the unloaded plate to check whether residual stresses, possibly introduced by manufacturing of the plate, could have some influence on the identification results. For this, the set of experimental natural frequencies given in Table 3 were used in the optimization procedure, assuming equal weighting factors  $W_p$  in Eq. (29). The optimization computations were carried-out by using the Sequential Quadratic Programming algorithm available in the MATLAB<sup>®</sup> *Optimization Toolbox*. At the end of 12 iterations, the identification results obtained were those presented in Table 3, in which the “Identified” natural frequencies correspond to the values predicted by the model derived by the Assumed Modes method acted upon by the identified stress field.

Table 3. Results for the first identification test

	Natural frequencies (Hz)						Force (N)
	1	2	3	4	5	6	
<b>Experimental</b>	113.75	152.50	290.00	322.50	368.75	533.75	0
<b>Identified</b>	116.66	148.72	291.96	321.57	368.86	531.06	0
<b>Error (%)</b>	2.56	-2.48	0.68	-0.29	0.03	-0.50	0

In a second identification test, the plate was loaded by applying a force of 190.3 N. The set of experimental natural frequencies given in Table 4 was used in the optimization procedure assuming equal weighting factors  $W_p$  in Eq. (29). As in the first identification test, the optimization computations were carried-out by using the Sequential Quadratic Programming. At the end of 8 iterations, the identification results obtained were those presented in Table 4.

Table 4. Results for the second identification test

	Natural frequencies (Hz)						Force (N)
	1	2	3	4	5	6	
<b>Experimental</b>	126.25	158.75	302.50	328.75	370.00	541.25	190.3
<b>Identified</b>	126.25	156.99	295.94	334.88	381.67	539.52	192.0
<b>Error (%)</b>	0.00	-1.11	-2.17	1.86	3.16	-0.32	0.91

The results presented above show that, in both identification tests, reasonably accurate results could be obtained. This demonstrates that the suggested identification procedure is robust with respect to measurement and modeling uncertainties.

## 9. Discussion and conclusions

As demonstrated in a number of previous studies, stress-stiffening can be generated either by stresses induced by external loads or by residual stresses produced by thermo-mechanical manufacturing processes. The numerical and experimental results presented in the previous sections clearly demonstrate that the stress-stiffening effect can have a significant influence upon the flexural dynamic behavior of thin rectangular plates. As a result, this effect should be accounted for in the modeling of vibrating systems in order to ensure the predictive capability of the models. Also, in dealing with the adjustment of finite element models based on experimental dynamic responses, the stress-stiffening effect must be taken into account since it can be responsible, at least partially, for the observed differences between model-predicted and experimentally-measured dynamic responses.

As in any inverse problem, the identification procedure presented in this paper exhibits some inherent difficulties that must be properly dealt with in practical applications: the identification can fail due to the existence of local minima of the objective function; the presence of experimental noise and model uncertainties can lead to biased solutions; uniqueness of the solution is not always guaranteed.

The results obtained in a number of applications using both numerically simulated and experimental data confirm the possibility of obtaining the external load or the stress-state within the structure by means of an inverse procedure. Clearly, such possibility depends on the availability of an adequate model to represent the stress-state. Ideally, this model should be accurate enough to represent the actual stress distribution and contain a reduced number of unknown parameters to be identified. In simple cases, such a model can be obtained by approximating an Airy's stress function by polynomial functions, as suggested in Section 3. For more complex cases, an alternative would be to use a base-line finite element model to represent the stress distributions, as suggested in Section 4 and then to identify scaling factors to be applied to the magnitudes of the loads used in the base-line model.

## 10. Acknowledgements

The authors gratefully acknowledge agencies CNPq of the Brazilian Ministry of Science and Technology and CAPES of the Brazilian Ministry of Education for the grant of Ph.D. and research scholarships.

## 11. References

- Almeida, S.F.M., Hansen, J.S., 1999, "Natural Frequencies of Composites Plates with Tailored Thermal Residual-Stresses", *International Journal of Solids and Structures*, Vol. 36, pp. 3517-3539.
- Craig Jr., R.R., 1981, "Structural Dynamics: an Introduction to Computer Methods", John Wiley.
- Donadon, M.V., Almeida, S.F.M., Faria, A. R., 2002, "Stiffening Effects on the Natural Frequencies of Laminated Plates with Piezoelectric Actuators", *Composites: Part B*, vol. 33, pp. 335-342.
- Géradin, M., Rixen, D., 1997, "Mechanical Vibrations – Theory and Application to Structural Dynamics", second edition, Wiley.
- Lieven, N.A.J., Greening, P.D., 2001, "Effect of Experimental Pre-Stress and Residual Stress on Modal Behavior", *Phil. Trans. R. Soc. London*, vol. 359, pp. 97-111.
- Kaldas, M.M., Dickinson, S.M., 1981, "The Flexural Vibration of Welded Rectangular Plates", *Journal of Sound and Vibration*, 75(2), pp. 163-178.
- Mead, D.J., 2003, "Vibration and Buckling Behavior of Flat Free-Free Plates Under Non-Uniform In-Plane Thermal Stresses", *Journal of Sound and Vibration*, n. 260, pp. 141-165.
- Rojas, J. E., Viana, F. A.C., Rade, D.A., Steffen Jr., V., 2004, "Identification of External Loads in Mechanical Systems Through Heuristic-Based Optimization Methods and Dynamic Responses", *Latin American Journal of Solids and Structures*, v. 1, n. 3, pp. 297-318.
- Rojas, J.E., 2004, "Characterization of Stress-stiffening Effect and Identification of Loads in Structures from Dynamic Responses" (in Portuguese), M.Sc. Dissertation, Federal University of Uberlândia, School of Mechanical Engineering.
- Simons, D.A., Leissa, A.W., 1971, "Vibrations of Rectangular Cantilever Plates Subjected to In-Plane Acceleration Loads", *Journal of Sound and Vibration*, vol. 17, n. 3, pp. 407-422.
- Timoshenko, S., Goodier, J.N., 1970, "Theory of Plates and Shells", McGraw-Hill Book.
- Young, D., 1950, "Vibration of Rectangular Plates by the Ritz Method", Annual Conference of the Applied Mechanics Division, Purdue University, Lafayette.

## 12. Responsibility notice

The authors are the only responsible for the printed material included in this paper.